Performance Analysis and Odometry Improvement of an Omnidirectional Mobile Robot for Outdoor Terrain

Genya Ishigami, Elvine Pineda, Jim Overholt, Greg Hudas, and Karl Iagnemma

Abstract—In this paper an omnidirectional mobile robot that possesses high mobility in rough terrain is presented. The omnidirectional robot has four active split offset caster (ASOC) modules, enabling the robot to move in any planar direction. It also possesses passive suspension articulation, allowing the robot to conform to uneven terrain. The agility of the robot is experimentally evaluated in various configurations. In addition, an odometry method that mitigates position estimation error due to wheel slippage is proposed. A key aspect of the proposed method is to utilize sensory data of wheel velocity, and turning rate around each ASOC pivot shaft, along with kinematic constraints of the robot configuration. Experimental odometry tests with different maneuvers in rough terrain are presented that confirm the utility of the proposed method.

I. INTRODUCTION

A N omnidirectional vehicle is able to kinematically move in arbitrary directions regardless of its current pose. Omnidirectional vehicles have been investigated [1]-[3] and widely applied in many practical areas, including mobile robotic bases for research, materials handling vehicles (i.e. fork trucks) for logistics, and wheelchairs. Most vehicles employ a specialized wheel design [4]-[7], which can become fouled during operation in rough, outdoor terrain. Also, specialized wheel designs often employ sub-rollers with small radii, leading to high ground pressure and sinkage in soft soils.

In this paper, an omnidirectional mobile robot driven by four active split offset caster (ASOC) modules is described (Fig. 1). The ASOC module consists of dual wheels with two freely rotatable axes around pivot (i.e. yaw) and roll, enabling the robot to drive/steer in any planar direction on rough terrain. The mobility of the robot is evaluated based on a metric defined as an omnidirectional mobility index.

The ASOC driven omnidirectional mobile robot can perform complex maneuvers (i.e. extremely sharp turning) that cannot be achieved by typical Ackermann steered wheeled vehicles. Such maneuvers require the robot to rapidly change wheel velocity, generating wheel slippage. Therefore, a key challenge described in this paper is to accurately estimate the position of the robot during wheel slippage.

Fig. 1. Omnidirectional mobile robot (left) and ASOC module (right)

There have been many research and development efforts devoted to position estimation techniques for mobile robots. A well-known technique is to simply employ GPS; however, GPS signals are not available in wooded or indoor areas due to blocked signals or multipath problems.

Another common technique for position estimation is odometry [8][9]. Odometry relies on wheel rotation data measured through encoders to estimate changes in the robot position over time. However, wheel slippage induces a miscount of wheel rotation, potentially resulting in significant position estimation error. Visual odometry has also been investigated for position estimation [10]-[12]. Visual odometry exploits consecutive images taken by a camera mounted on the robot to estimate the distance traveled. This technique is relatively robust for most terrain types. However, visual odometry requires implementation of a relatively complex image processing algorithm.

To achieve accurate position estimation with simple, internal sensors, this paper proposes an odometry method that can partially compensate for estimation error due to wheel slippage. The method estimates wheel slippage based on the sensory data obtained from wheel angular velocity and turning rate around the ASOC pivot shaft.

Experimental odometry tests are conducted for two different omnidirectional maneuvers under various traveling velocities. Position estimation errors based on the proposed odometry method is then evaluated for each test run.

This paper is organized as follows: Section II introduces a system overview of the ASOC-driven omnidirectional mobile robot. Section III describes the kinematic control of the robot. Mobility evaluation based on the omnidirectional mobility index is summarized in Section IV. The proposed odometry method with slip compensation is presented in Section V, and experimental validation of the odometry method is summarized in Section VI.

1. REPORT DATE **SEP 2011**	2. REPORT TYPE	3. DATES COVERED **00-00-2011 to 00-00-2011**

4. TITLE AND SUBTITLE	5a. CONTRACT NUMBER
Performance Analysis and Odometry Improvement of an Omnidirectional Mobile Robot for Outdoor Terrain	5b. GRANT NUMBER
	5c. PROGRAM ELEMENT NUMBER
6. AUTHOR(S)	5d. PROJECT NUMBER
	5e. TASK NUMBER
	5f. WORK UNIT NUMBER

7. PERFORMING ORGANIZATION NAME(S) AND ADDRESS(ES) **Massachusetts Institute of Technology (MIT),Department of Mechanical Engineering,Cambridge,MA,02139**	8. PERFORMING ORGANIZATION REPORT NUMBER

9. SPONSORING/MONITORING AGENCY NAME(S) AND ADDRESS(ES)	10. SPONSOR/MONITOR'S ACRONYM(S)
	11. SPONSOR/MONITOR'S REPORT NUMBER(S)

12. DISTRIBUTION/AVAILABILITY STATEMENT
Approved for public release; distribution unlimited

13. SUPPLEMENTARY NOTES

14. ABSTRACT
In this paper an omnidirectional mobile robot that possesses high mobility in rough terrain is presented. The omnidirectional robot has four active split offset caster (ASOC) modules, enabling the robot to move in any planar direction. It also possesses passive suspension articulation, allowing the robot to conform to uneven terrain. The agility of the robot is experimentally evaluated in various configurations. In addition an odometry method that mitigates position estimation error due to wheel slippage is proposed. A key aspect of the proposed method is to utilize sensory data of wheel velocity, and turning rate around each ASOC pivot shaft, along with kinematic constraints of the robot configuration. Experimental odometry tests with different maneuvers in rough terrain are presented that confirm the utility of the proposed method.

15. SUBJECT TERMS

16. SECURITY CLASSIFICATION OF:			17. LIMITATION OF ABSTRACT	18. NUMBER OF PAGES	19a. NAME OF RESPONSIBLE PERSON
a. REPORT **unclassified**	b. ABSTRACT **unclassified**	c. THIS PAGE **unclassified**	**Same as Report (SAR)**	**6**	

Standard Form 298 (Rev. 8-98)
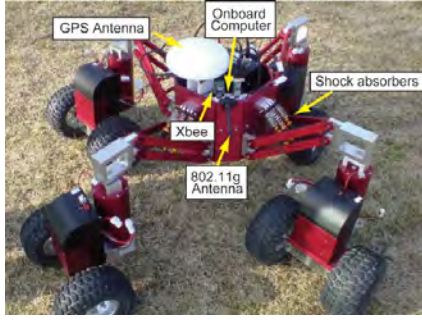Prescribed by ANSI Std Z39-18

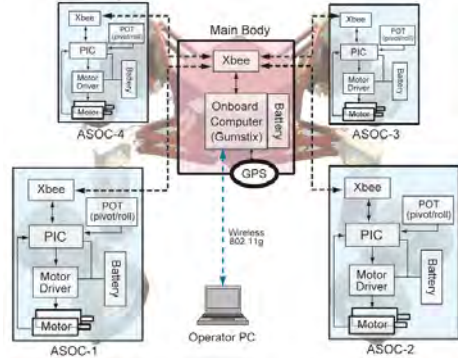Fig. 2. Omnidirectional mobile robot with experimental setup

Fig. 3. Robot schematic diagram. Dotted lines indicate wireless communication links.

II. ASOC-DRIVEN OMNIDIRECTIONAL MOBILE ROBOT

A. System Overview

The omnidirectional mobile robot (Fig. 2) consists of a main body and four ASOC modules. Each ASOC module is connected to the body via a parallel linkage with shock absorbers. The robot's maximum dimension is 112 x 112 x 39 cm and the weight is 35 kg. The maximum cruising velocity is 2.2 m/s (8.0 km/h).

Fig. 3 shows a schematic diagram of the robot. The onboard computer (Gumstix Overo Earth) is mounted on the main body, working as a central computing device. The onboard computer supervises all ASOC modules via Xbee wireless links, such that the onboard computer kinematically coordinates ASOC modules to move the robot in a desired direction. GPS data is collected as ground truth data for outdoor experiments. These data are sent to an operator via IEEE 802.11g, along with ASOC motion data (i.e. potentiometer for pivot angle and wheel tachometer data).

B. Active Split Offset Caster Module Description

The ASOC module consists of a split wheel pair, connecting axle, and offset link connected to the wheel pair (Fig. 4). Based on the kinematic isotropy analysis reported in [13][14], the geometric ratio L_{split}/L_{offset} is designed to be 2.0 for the most isotropic mobility the ASOC. The wheel pair/axle assembly passively rotates around the pivot axis. The roll axis also passively rotates, maintaining wheel contact on sloped or rough terrain surfaces. The angle of rotation of the pivot and roll axes are measured by potentiometers.
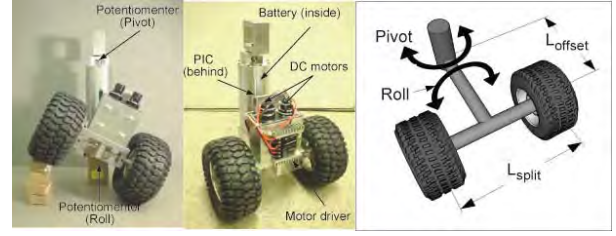

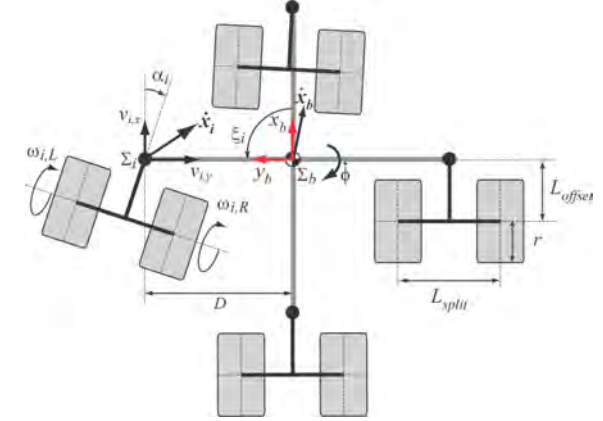Fig. 4. Assembly of Active Split Offset Caster module.

Fig. 5. Kinematic model of the ASOC-driven omnidirectional mobile robot.

TABLE I
KINEMATIC PARAMETERS FOR OMNIDIRECTIONAL MOBILE ROBOT

Symbol	Value
D	0.353 m
L_{offset}	0.110 m
L_{split}	0.228 m
R	0.085 m
ξ_i	$[0, 0.5\pi, \pi, 1.5\pi]$

For omnidirectional motion, each ASOC module can produce planar translational velocities at a point along its pivot axis by independently controlling each wheel's velocity. A control method is presented in Section III-B.

Each ASOC module is a self-sustained robotic system, comprised of a power supply, actuators, microcontroller (PIC), wireless device, and motor driver. Each module performs simple tasks assigned by the supervisory computer on the body, and executes local feedback control.

III. KINEMATIC CONTROL OF OMNIDIRECTIONAL ROBOT

A. Kinematic Model

Fig. 5 illustrates a kinematic model of the ASOC-driven omnidirectional mobile robot. The coordinate frame for the main body Σ_b is fixed on the body centroid and defined as a right-hand frame, depicting the longitudinal direction as x. The coordinate frame for each ASOC module Σ_i (i=1…4) is defined such that the z axis is aligned to the pivot shaft and fixed at a point along its pivot axis. (Σ_i does not rotate along with the ASOC rotation around its pivot axis.) D and ξ_i locate each ASOC module with regard to the main body, and r is the wheel radius. Table I summarizes kinematic parameters that are used in the experiments described later.

B. Kinematic Control

The kinematic control method described here calculates all wheel angular velocities that satisfy desired body translational and rotational velocities defined in an inertial coordinate frame. First, the velocity of the ASOC module can be calculated as:

$$\dot{\boldsymbol{x}}_i = \begin{bmatrix} v_{i,x} \\ v_{i,y} \end{bmatrix} = \dot{\boldsymbol{x}}_b + \dot{\phi} D \begin{bmatrix} \cos \xi_i \\ \sin \xi_i \end{bmatrix} \quad (i = 1...4) \qquad (1)$$

where $\dot{\boldsymbol{x}}_i$ and $\dot{\boldsymbol{x}}_b$ are the planer velocity vectors at the i-th ASOC coordinate frame Σ_i and body frame Σ_b, respectively. $\dot{\phi}$ is the yaw rate of the main body. For kinematic control, $\dot{\boldsymbol{x}}_b$ and $\dot{\phi}$ are the input variables given by an operator.

The wheel angular velocities, $\omega_{i,L}$ and $\omega_{i,R}$, that yield the desired i-th ASOC planer velocity are formulated as follows:

$$\begin{bmatrix} \omega_{i,L} \\ \omega_{i,R} \end{bmatrix} = \frac{C^{-1} \dot{\boldsymbol{x}}_i}{r} \qquad (2)$$

C is a coordinate transformation matrix, written as:

$$C = \frac{1}{2} \begin{bmatrix} \cos \alpha_i + 2L\sin \alpha_i & \cos \alpha_i - 2L\sin \alpha_i \\ \sin \alpha_i - 2L\cos \alpha_i & \sin \alpha_i + 2L\cos \alpha_i \end{bmatrix} \qquad (3)$$

where, α_i is the angle of the pivot axis, measured by the potentiometer, and $L = L_{offset}/L_{split}$. The wheel angular velocity obtained from the above equations is then achieved via simple PID feedback control.

Note that the control method described above aligns the thrust vector of each ASOC in the desired direction of travel, minimizing energy loss caused by internal forces.

IV. OMNIDIRECTIONAL MOBILITY TEST

A. Omnidirectional Mobility Index

Several metrics have been proposed for mobility analysis of mobile vehicles in rough terrain. For example, a mobility index for off-road vehicle based on factors such as contact pressure and weight was proposed in [15]. Another metric based on body motion (i.e. velocity, acceleration, or jerk) is commonly used to evaluate the mobility of passenger vehicles or mobile robots.

Focusing on the mobility of omnidirectional vehicles, a particular requirement is high agility for a near-arbitrary omnidirectional maneuver. In the case of an ASOC-driven omnidirectional mobile robot, each ASOC needs to be kinematically coordinated in order to perform a given maneuver. Thus, in this work, a metric related to the ASOC motion is employed for mobility evaluation. The metric, termed an omnidirectional mobility index, is defined as the root mean square error (Fig. 6) between the desired profile of the ASOC pivot angle and its actual profile measured by a potentiometer on its axis. The index has a unit of degrees. The smaller the magnitude of the index, the more agile the omnidirectional vehicle. A net omnidirectional mobility index of the robot can be computed as a mean value between the indices obtained from four ASOC modules.
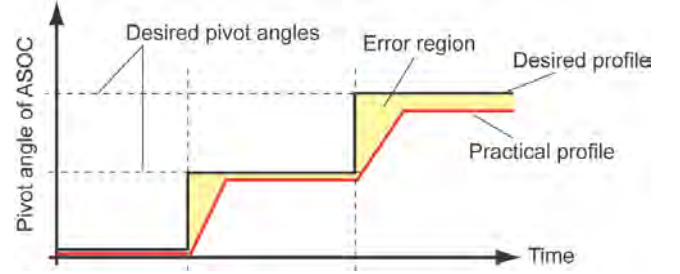

Fig.6. Schematic graph for a time history of the pivot angle of an ASOC module. The black line is the desired profile (given maneuver) and the red line is the measured profile (actual maneuver). The yellow region indicates error between the desired and measured pivot angle.

B. Experimental Description

Two different robot configurations have been experimentally tested: in Configuration 1 the velocity vector of the robot is always aligned with the orientation of the ASOC modules (i.e. a cross-shape configuration); in Configuration 2 the velocity vector of the robot is diagonal (45 degrees) with regard to ASOC module orientation (i.e. X-shape configuration).

During the experimental test the robot changes its velocity vector by 90 degrees every 5 seconds, resulting in a square motion path. The traveling velocity of the robot is controlled to maintain a constant value of 0.36 m/s. Each ASOC module calculates the wheel angular velocity required for the maneuver based on the kinematic control method as described in Section III-B.

The effect of suspension design on omnidirectional mobility is examined by comparing the results from the vehicle with a standard, compliant suspension to results from the vehicle with a suspension composed of rigid links.

C. Experimental Results

Fig. 7 shows a time history of the pivot angle in Configurations 1 and 2 with and without compliant suspension, respectively. Also, the omnidirectional mobility index for each configuration is summarized in Table II.

Comparing the graphs and table, the omnidirectional mobility indices between the two configurations is negligible: it is less than 0.1 degrees in the case of the robot without compliant suspension, and 1.6 degrees with. This suggests that the ASOC-driven omnidirectional robot has relatively high agility that is independent of configuration.

In addition, it can be seen that the omnidirectional mobility of the robot with rigid links (without compliant suspension) is better than the robot with compliant suspension. This is due to the fact that the suspension's shock absorbers mitigate sudden velocity change by dissipating energy. The shock absorbers also reduce thrust energy generated at the wheel contact patches while turning, resulting in a less agile turning motion.

On the other hand, the system with rigid links can efficiently coordinate each ASOC with less energy loss, enabling more agile maneuver. This result implies that a trade-off between high terrain adaptability (with compliant suspension) and high omnidirectional mobility (with rigid links) is needed.

a)   w/o compliant suspension   b)   w/ compliant suspension

(Configuration 1)

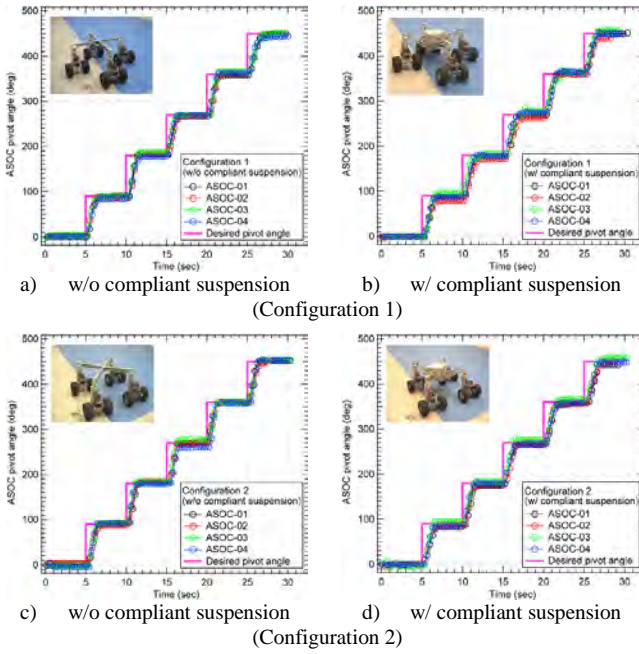c)   w/o compliant suspension   d)   w/ compliant suspension

(Configuration 2)

Fig. 7. Time history of the pivot angle for mobility evaluation

TABLE II
OMNIDIRECTIONAL MOBILITY INDEX AT EACH CONFIGURATION
WITH/WITHOUT COMPLIANT SUSPENSIONS (UNIT IS DEGREES).

Configuration 1		Configuration 2	
w/o compliant suspension	w/ compliant suspension	w/o compliant suspension	w/ compliant suspension
29.91	33.43	29.84	31.82

V. ODOMETRY FOR OMNIDIRECTIONAL MOBILE ROBOT

The proposed odometry method includes two key approaches to improving odometry performance: 1) an odometry calculation that enforces the robot's kinematic constraints to reduce error due to kinematic parameter uncertainty, and 2) wheel slip compensation by the ASOC module.

A. Odometry Using Kinematic Constraints

An odometry method for the ASOC-driven omnidirectional mobile robot is described as follows: First, the wheel angular velocities of each ASOC [$\omega_{i,L}$, $\omega_{i,R}$] and the pivot angle α_i are measured by the tachometers and potentiometer, respectively. Subsequently, from (1) to (3), the translational velocity of the body can be estimated using the measured wheel velocity and pivot angle as follows:

$$\dot{x}_b = \dot{x}_i - \dot{\phi} \cdot D \begin{bmatrix} \cos \xi_i \\ \sin \xi_i \end{bmatrix}$$
$$= C(\alpha_i) \cdot r \cdot \begin{bmatrix} \omega_{i,L} \\ \omega_{i,R} \end{bmatrix} - \dot{\phi} \cdot D \begin{bmatrix} \cos \xi_i \\ \sin \xi_i \end{bmatrix} \qquad (4)$$

The above equation indicates that the body velocity can be calculated by data obtained from each ASOC, which means that the robot is kinematically redundant. Therefore, using four sets of ASOC data, a body velocity can be estimated via an appropriate filter, such as a mean filter, median filter, or

others. In the experiments described later, the body velocity is obtained as the mean value of the velocities estimated from individual ASOCs:

$$\dot{x}_b = \frac{1}{4} \sum_{i=1}^{4} \left(C(\alpha_i) \cdot r \cdot \begin{bmatrix} \omega_{i,L} \\ \omega_{i,R} \end{bmatrix} - \dot{\phi} \cdot D \begin{bmatrix} \cos \xi_i \\ \sin \xi_i \end{bmatrix} \right) \qquad (5)$$

The yaw rate of the body $\dot{\phi}$ is also given as follows:

$$\dot{\phi} = \frac{1}{4D} \sum_{i=1}^{4} \left(v_{i,y} \cos \xi_i - v_{i,x} \cos \xi_i \right) \qquad (6)$$

Finally, the position and heading of the omnidirectional robot is estimated by the time integrals of $\dot{x}_b$ and $\dot{\phi}$ at sequential sampling time steps.

B. Wheel Slip Compensation

As described in Section I, position estimation based on traditional odometry methods may not be accurate in rough terrain. This is due to wheel slippage that causes miscounts of wheel rotation. In particular, the ASOC-driven omnidirectional mobile robot experiences large wheel slippage during sharp turning maneuvers.

The basic idea of slip compensation is to exploit sensory data only obtained from wheel angular velocity and pivot turning rate. The pivot turning rate $\dot{\alpha}_i$ is calculated from time series data of the potentiometer mounted on the pivot shaft. It is also estimated as the difference between the left and right wheel circumference velocity (v_R and v_L, Fig. 8):

$$\dot{\alpha}_{i,w} = (v_R - v_L) / L_{split} = r(\omega_{i,R} - \omega_{i,L}) / L_{split} \qquad (7)$$

However, the wheel circumference velocity calculated from the tachometer is not equivalent to the true ground speed of the wheel because of wheel slippage.

Assuming that the slip velocity Δv_s is generated at each wheel with the same magnitude but opposite direction, the true ground speeds of each wheel, $\hat{v}_R$ and $\hat{v}_L$, are modeled as:

$$\hat{v}_R = v_R - \Delta v_s$$
$$\hat{v}_L = v_L + \Delta v_s \qquad (8)$$

Also, the pivot turning rate $\dot{\alpha}_i$ measured by the potentiometer is equivalent to the value calculated by the true ground speed of the wheel:

$$\dot{\alpha}_i = (\hat{v}_R - \hat{v}_L) / L_{split} \qquad (9)$$
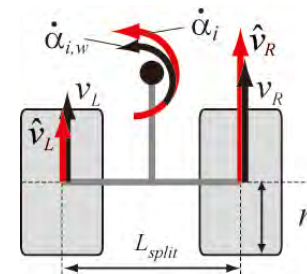

Fig. 8. Kinematic model of ASOC for wheel slip compensation. Red arrows indicate the wheel ground speed and true pivot turning rate. Black arrows indicate the wheel speed and pivot rate measured by the tachometer.

Therefore, subtracting (9) from (7), the slip velocity Δv_s can be estimated as follows:

$$\Delta v_s = (\dot{\alpha}_{i,w} - \dot{\alpha}_i)L_{split}/2 \qquad (10)$$

Finally, the true ground speed of the wheel is calculated by substituting (10) to (8). This is then used for the odometry calculations in (5) and (6).

The method described above uses only two sensors implemented on the ASOC, and does not need additional sensors for the slip compensation. This method is relatively simple but shows reasonably good improvement, as summarized in Section VI.

VI. ODOMETRY EXPERIMENTAL RESULTS

A. Experimental Setup and Condition

In this experiment, the omnidirectional mobile robot is controlled to execute two pre-defined maneuvers: Maneuver 1 increments the velocity vector of the robot by 90 degrees every 10 seconds; Maneuver 2 increments the velocity vector of the robot 30 degrees every 3 seconds. Two different traveling velocities, 0.36 m/s and 0.60 m/s, are also tested in each maneuver. Four different conditions have been tested in total. The test field is a bumpy, grass-covered outdoor field.

The following data are measured during each experimental run: pivot turning angles, wheel angular velocities, and GPS data of the robot position as ground truth. The accuracy of the GPS sensor is 0.12 m in horizontal using code-based differential positioning as its specification reported in [16].

The experimental data sets at each run are stored in the onboard computer and used for post-processed odometry analysis. In order to evaluate the proposed odometry method, the odometry with slip compensation is compared to the method which does not consider slip compensation.

B. Experimental Results

Fig. 9 and Fig. 10 show the results of the odometry analyses. In the figure, the ground truth of the robot motion path measured by GPS is drawn as a black dotted line. Paths estimated by odometry with and without slip compensation are drawn as red and black solid lines, respectively. Table III summarizes the error between the position estimates based on odometry and the ground truth. The errors are evaluated by both root mean square (RMS) error over the path, and the final straight-line error between the true and estimated robot terminal points. The error percentage for the final state is calculated by dividing the error value by the total distance traveled.

In each run, the wheel velocity was controlled to follow a sequential pre-defined maneuver, but the position of the robot was not controlled (i.e. no path following control was used). Therefore, the motion of the robot consists of distorted curves because of terrain roughness and wheel slippage.

In Maneuver 1, the odometry with slip compensation estimates the robot position with an error of less than 6 %. This result confirms that the proposed method can reasonably compensate for wheel slippage generated at sharp turning maneuvers on each square corner.

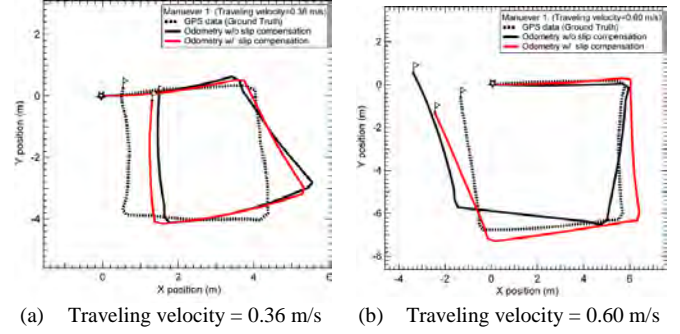(a) Traveling velocity = 0.36 m/s (b) Traveling velocity = 0.60 m/s

Fig. 9. Experimental results of position estimation based on odometry (Maneuver 1, square motion). A star icon on the figure indicates the start point, and flag icons describe the final position of the ground truth and estimated paths, respectively.
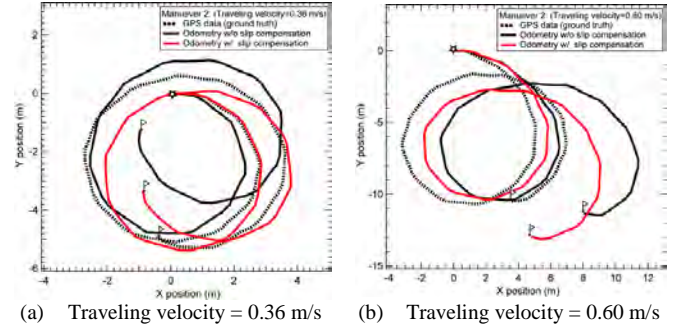

(a) Traveling velocity = 0.36 m/s (b) Traveling velocity = 0.60 m/s

Fig. 10. Experimental results of position estimation based on odometry (Maneuver 2, circular motion).

TABLE III
POSITION ESTIMATION ERROR

Maneuver 1	w/o slip compensation		w/ slip compensation	
Velocity	RMS error	Final state error	RMS error	Final state error
0.36 m/s	0.98	1.19 (7.3 %)	0.83	0.92 (5.7 %)
0.60 m/s	1.16	2.40 (9.8 %)	0.66	1.31 (5.4 %)

Maneuver 2	w/o slip compensation		w/ slip compensation	
velocity	RMS error	Final state error	RMS error	Final state error
0.36 m/s	1.42	3.65 (13.0 %)	0.87	1.63 (5.8 %)
0.60 m/s	3.12	4.63 (10.7 %)	2.51	2.75 (6.4 %)

(Unit is meters, and percentages for the final state error are in parentheses.)

In Maneuver 2, the accuracy of the odometry without slip compensation is more than 10 %. This is likely because the changes in wheel velocity in Maneuver 2 are more frequent (3 sec interval) than in Maneuver 1 (10 sec interval), thus increasing the chance of wheel slippage in Maneuver 2 when the robot changes its traveling direction.

Despite the longer distance traveled and high slip motion in Maneuver 2, the proposed odometry method with slip compensation can estimate the motion with reasonable accuracy (approximately 6 % of distance traveled). This result also suggests that, for the robot platform tested here, the proposed method can estimate the position with similar accuracy independent of the nature of the maneuver and the traveling velocity.
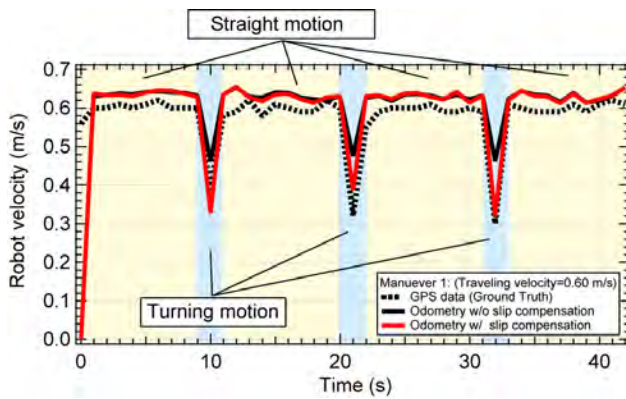
Fig. 11. Time history of the robot traveling velocity (Maneuver 1 with traveling velocity of 0.60 m/s)

C. Discussion on Observed Odometry Error

In the experiment, it was observed that wheel slippage is also constantly generated even when the robot is traveling along a straight path. This constant wheel slippage cannot be compensated by the proposed method because the pivot turning rate will be very small in such a maneuver.

Fig. 11 shows a time history of the robot traveling velocity. The black dotted line is the velocity measured by GPS. The red and black lines are the velocities estimated by odometry with and without slip compensation, respectively. From the graph, the proposed method yields a good estimate of the traveling velocity during turning motion (every 10 seconds), when compensating for wheel slippage. However, wheel slippage during straight motion (5–12% of the true traveling velocity) was not compensated by either odometry method. This constant wheel slippage is likely due to the (semi-) deformable rough terrain that the experiment was performed on. An estimation of constant wheel slippage in rough terrain will be necessary for more robust odometry, as reported in [17][18]. In addition, estimation error of the traveling velocity is also due to the fact that the wheel is deformable, resulting in varied wheel radius during travel. To deal with the uncertainty of the wheel radius, a Kalman filter could be employed such that the position estimate is given along with error ellipses due to the varied wheel radius.

VII. CONCLUSION

In this paper, an ASOC-driven omnidirectional mobile robot that possesses high agility has been presented. A system overview of the robot and the ASOC module has been introduced, along with a kinematic control scheme for the robot. The agility of the robot has been evaluated based on the omnidirectional mobility index. Mobility tests confirm that the omnidirectional mobile robot has an ability to move in any direction regardless of its configuration. The experimental results imply that an optimization of the suspension properties will be necessary to yield better terrain adaptation as well as higher agility.

A simple slip-compensation odometry method has been also proposed in this paper. The odometry method consists of two key approaches: kinematic constraint enforcement and wheel slip compensation. Experimental tests with two different maneuvers were conducted on outdoor terrain, and the results confirm that the proposed odometry can estimate the position of the robot within an error of 5–6% of total distance traveled, regardless of given traveling velocity and maneuvers.

Further improvement of the odometry method will include an estimation of constant wheel slippage observed during straight-line travel of the robot, and uncertainty compensation of the kinematic parameters of the robot.

REFERENCES

[1] P. Muir and C. Neuman, "Kinematic Modeling for Feedback Control of an Omnidirectional Wheeled Mobile Robot," in *Proc. the 1987 IEEE Int. Conf. on Robotics and Automation*, Raleigh, NC, pp. 1772–1778.

[2] S. Fujisawa, K. Ohkubo, T. Yoshida, N. Satonaka, Y. Shidama, and H. Yamaura, "Improved Moving Properties of an Omnidirectional Vehicle Using Stepping Motor," in *Proc. the 36th Conf. on Decision and Control*, San Diego, CA, 1997, pp.3654–3657.

[3] R. Williams, B. Carter, P. Gallina, and G. Rosati, "Wheeled Omni-directional Robot Dynamics Including Slip," in *Proc. the 2002 ASME Design Engineering Technical Conf.*, Montreal, Canada, pp. 201–207.

[4] B. E. Ilon, "Wheels for a course stable self-propelling vehicle movable in any desired direction on the ground or some other base," 1975, US Patent 3,876,255.

[5] F.G. Pin and S.M. Killough, "A New Family of Omnidirectional and Holonomic Wheel Platforms for Mobile Robots," *IEEE Trans. on Robotics and Automation*, vol. 10, no. 4, pp. 480–489, 1994.

[6] M. West and H. Asada, "Design of Ball Wheel Mechanisms for Omnidirectional Vehicles with Full Mobility and Invariant Kinematics," *ASME Journal of Mechanical Design*, vol. 117, no. 2, pp.153-161, 1997.

[7] L. Ferriere and B. Raucent, "ROLLMOBS, A New Universal Wheel Concept," in *Proc. the 1998 Int. Conf. on Robotics and Automation*, Leuven, Belgium, pp. 1877-1882.

[8] J. Borenstein and L. Feng, "Measurement and correction of systematic odometry errors in mobile robots," *IEEE Trans. on Robotics and Automation*, vol. 12, no. 6, pp. 869–880, Dec. 1996.

[9] J. Borenstein, "Experimental Results from Internal Odometry Error Correction with the OmniMate Mobile Robot," *IEEE Trans. on Robotics and Automation*, vol. 14, no. 6, pp. 963–969, Dec. 1998.

[10] D. Nister, O. Naroditsky, and J. Bergen, "Visual odometry," in *Proc. IEEE Computer Society Conf. on Computer Vision and Pattern Recognition*, Washington DC, 2004, pp. 652–659.

[11] M. Maimone, Y. Cheng, L. Matthies, "Two years of Visual Odometry on the Mars Exploration Rovers," *Journal of Field Robotics*, vol. 24, no. 3, pp.169–186, Mar. 2007.

[12] K. Nagatani, A. Ikeda, G. Ishigami, K. Yoshida, and I. Nagai, "Development of a Visual Odometry System for a Wheeled Robot on Loose Soil Using a Telecentric Camera," *Advanced Robotics*, vol. 24, no. 8-9, pp. 1149–1167, May 2010.

[13] M. Udengaard and K. Iagnemma, "Design of an Omnidirectional Mobile Robot for Rough Terrain," in *Proc. 2008 IEEE Int. Conf. on Robotics and Automation*, Pasadena, CA, pp. 1666–1671.

[14] K. Iagnemma, M. Udengaard, G. Ishigami, M. Spenko, S. Oncu, I. Khan, J. Overholt, and G. Hudas, "Design and Development of an Agile, Man Portable Unmanned Ground Vehicle," in *Proc. the 26th Annual Army Science Conference*, Orlando, FL, E0-04, 2008.

[15] J. Wong, *Theory of Ground Vehicles. 4th Ed*, New York, Wiley, 2008.

[16] NavCom Technology Inc., SF-2050 GPS Product User Guide, available from http://www.navcomtech.com/Support/, (as of March 2010).

[17] L. Ojeda, D. Cruz, G. Reina, and J. Borenstein, "Current-based slippage detection and odometry correction for mobile robots and planetary rovers," *IEEE Trans. on Robotics*, vol. 22, no. 2, pp. 365–377, 2006.

[18] C. Ward and K. Iagnemma, "A Dynamic-Model-Based Wheel Slip Detector for Mobile Robots on Outdoor Terrain," *IEEE Trans. on Robotics*, vol. 24, no. 4, pp. 821-831, 2008.